

# The Two-flux Composite Fermion Series of Fractional Quantum Hall States in Strained Si

K. Lai,<sup>1</sup> W. Pan,<sup>2</sup> D.C. Tsui,<sup>1</sup> S. Lyon,<sup>1</sup> M. Muhlberger,<sup>3</sup> and F. Schaffler<sup>3</sup>

<sup>1</sup>*Department of Electrical Engineering, Princeton University, Princeton, New Jersey 08544*

<sup>2</sup>*Sandia National Laboratories, Albuquerque, NM 87185*

<sup>3</sup>*Institut für Halbleiterphysik, Universität Linz, Linz, Austria*

(Dated: September 17, 2018)

Magnetotransport properties are investigated in a high-mobility two-dimensional electron system in the strained Si quantum well of a (100) Si<sub>0.75</sub>Ge<sub>0.25</sub>/Si/Si<sub>0.75</sub>Ge<sub>0.25</sub> heterostructure, at temperatures down to 30mK and in magnetic fields up to 45T. We observe around  $\nu = 1/2$  the two-flux composite fermion (CF) series of the fractional quantum Hall effect (FQHE) at  $\nu = 2/3, 3/5, 4/7$ , and at  $\nu = 4/9, 2/5, 1/3$ . Among these FQHE states, the  $\nu = 1/3, 4/7$  and  $4/9$  states are seen for the first time in the Si/SiGe system. Interestingly, of the CF series, the  $3/5$  state is weaker than the nearby  $4/7$  state and the  $3/7$  state is conspicuously missing, resembling the observation in the integer quantum Hall effect regime that the  $\nu = 3$  is weaker than the nearby  $\nu = 4$  state. Our data indicate that the two-fold degeneracy of the CFs is lifted and an estimated valley splitting of  $\sim 1$  K.

PACS numbers: 73.43.Qt, 72.20.My, 73.63.Hs

The composite fermion (CF) model[1, 2, 3, 4, 5, 6] has been very successful in explaining the principal fractional quantum Hall effect (FQHE) sequences of  $\nu = p/(2p \pm 1)$  ( $p = 1, 2, 3, \dots$ ) around the Landau level filling  $\nu = 1/2$ . In this model, two fictitious flux quanta are attached to each electron. The so-formed new particles, composite fermions, can be treated as independent particles, and they move in a reduced effective magnetic ( $B$ ) field,  $B_{eff} = B - 2\pi h/e$ . At  $\nu = 1/2$ ,  $B_{eff} = 0$  and the CFs form a Fermi sea. When  $B_{eff}$  deviates from zero, Landau quantization of the cyclotron orbits of CFs breaks up the CF energy continuum into discrete Landau levels, giving rise to integer quantum Hall effect (IQHE) states. The IQHE of the CFs at filling factor  $p$  corresponds to the FQHE of the electrons at  $\nu = p/(2p \pm 1)$ .

So far, research on CFs has mainly been carried out in the two-dimensional electron system (2DES) in the lattice-matched GaAs/Al<sub>x</sub>Ga<sub>1-x</sub>As heterostructures. Applicability of the CF model in other material systems, especially the strained Si quantum well in the Si/Si<sub>1-x</sub>Ge<sub>x</sub> heterostructure, has not been tested experimentally. In comparison to the GaAs/AlGaAs systems, its multi-valley band structure, large electron effective mass and  $g$ -factor, and negligible spin-orbit interaction are expected to introduce new degrees of freedom into the CF physics. Over the past ten years, the quality of strained Si has been continuously improving[7, 8, 9] and a low-temperature 2DES mobility as high as  $\mu \sim 600,000$  cm<sup>2</sup>/Vs has recently been reported[10]. However, high magnetic field measurements at dilution refrigerator temperatures are lacking and very few FQHE states have so far been observed. In fact, to date, only the two FQHE states at  $\nu = 2/3$  and  $4/3$  are firmly established [11, 12, 13, 14, 15]. Worse yet, the most prominent  $\nu = 1/3$  FQHE state is still missing from observation and the question whether the FQHE sequences

in strained Si still follow the two-flux CF series has thus remained unanswered.

In this paper, we report the magnetotransport data in a high-mobility 2DES realized in the strained Si layer of a (100) Si<sub>0.75</sub>Ge<sub>0.25</sub>/Si/Si<sub>0.75</sub>Ge<sub>0.25</sub> quantum well structure at temperatures ( $T$ ) down to 30mK and in magnetic ( $B$ ) fields up to 45T. Around  $\nu = 1/2$ , we observe the principal FQHE states at  $\nu = 2/3, 3/5, 4/7$ , and at  $\nu = 4/9, 2/5, 1/3$  — the two-flux CF series. This result demonstrates that the CF model still applies in the Si/SiGe systems. Interestingly, of the  $p/(2p \pm 1)$  CF series, the  $3/5$  state is weak compared to the nearby  $4/7$  state and the  $3/7$  state is conspicuously missing, resembling the situation in the integer quantum Hall effect regime where the  $\nu = 3$  state, due to the small valley splitting, is weaker than the nearby  $\nu = 4$  state. In addition to the principal FQHE states, weak  $\rho_{xx}$  minima are also observed at  $\nu = 4/5$  and  $\nu = 8/11$  around the even denominator  $\nu = 3/4$  fraction, as well as the  $\nu = 4/3$  and  $8/5$  FQHE states between  $\nu = 1$  and 2. For  $\nu < 1/3$ , an insulating phase takes place and no FQHE states are seen. The energy gap of the  $\nu = 1/3$  FQHE state obtained from activation measurement is  $\Delta_{1/3} = 0.8$  K.

The specimen is an MBE grown, modulation doped n-type Si<sub>0.75</sub>Ge<sub>0.25</sub>/Si/Si<sub>0.75</sub>Ge<sub>0.25</sub> heterostructure. The strained Si quantum well is 15 nm wide. Details of the growth and the sample structure can be found in Ref. [9]. Ohmic contacts to the 2DES were made by evaporating Au/Au:Sb and annealing at 370°C in a forming gas atmosphere. At  $T \sim 30$  mK, the 2DES has a density  $n = 2.7 \times 10^{11}$  cm<sup>-2</sup> and mobility  $\mu = 250,000$  cm<sup>2</sup>/Vs, after low temperature illumination by a red light-emitting diode. Standard low-frequency ( $\sim 7$  Hz) lock-in techniques were used to measure the magnetoresistivity  $\rho_{xx}$  and the Hall resistivity  $\rho_{xy}$ .

Fig. 1 shows the  $\rho_{xx}$  and  $\rho_{xy}$  traces, taken at  $T = 30$

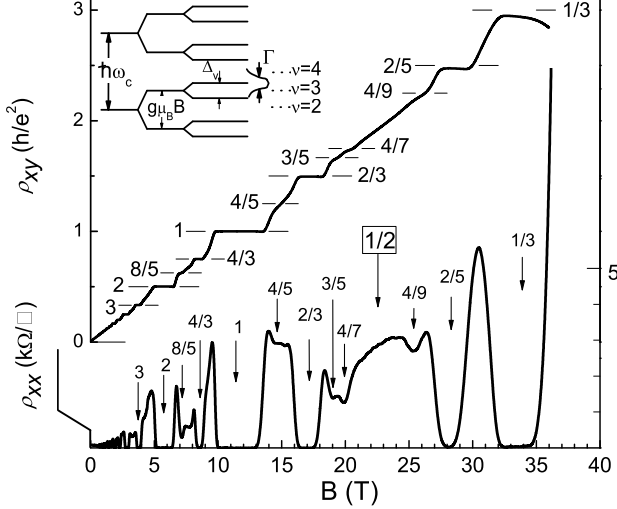


FIG. 1: Diagonal resistivity  $\rho_{xx}$  and Hall resistivity  $\rho_{xy}$  of the 2DES in a strained Si quantum well at  $T = 30\text{mK}$ . The 2DES has a density  $n = 2.7 \times 10^{11}\text{cm}^{-2}$  and mobility  $\mu = 250,000\text{cm}^2/\text{Vs}$ . Major fractional quantum Hall states are marked by arrows. The insert shows the electron Landau level diagram.  $\Gamma$  shows schematically the level broadening.

mK. In the low  $B$  field regime, the Shubnikov-de Haas oscillations are clearly resolved up to  $\nu = 36$ . The odd integer quantum Hall state, with an energy gap reflecting the small valley splitting of the 2D electrons, appears at as early as  $\nu = 11$ . These features manifest the high quality of our sample. Between  $\nu = 3$  and 4 and between  $\nu = 4$  and 5, noticeable  $\rho_{xx}$  dips are observed at  $\nu = 7/2$  and  $9/2$ . In the lowest Landau level between  $\nu = 1$  and 2, two FQHE states,  $8/5$  and  $4/3$ , are present. Similar to previous studies, the  $\nu = 5/3$  state is missing[13].

For  $\nu < 1$ , the FQHE states are observed at  $\nu = 1/3$ ,  $2/5$ ,  $4/9$ ,  $4/7$ ,  $3/5$ , and  $2/3$ . Weak  $\rho_{xx}$  minima are also observed at  $\nu = 4/5$  and  $8/11$ . Evidence of the  $\nu = 2/5$  FQHE state was first reported by Dunford *et al.* in Ref. [13]. However, only in this high quality sample the formation of the  $\nu = 2/5$  FQHE state is unambiguously established: Its  $\rho_{xx}$  is virtually zero within our experimental resolution and  $\rho_{xy}$  shows a well-developed plateau. The  $\nu = 4/7$  and  $\nu = 4/9$  states are seen for the first time. Interestingly, while the  $\nu = 4/7$  and  $4/9$  states show well-developed  $\rho_{xx}$  minima, the  $\nu = 3/5$  state is weaker than the nearby  $\nu = 4/7$  FQHE states and the  $\nu = 3/7$  state is missing. When  $\nu < 1/3$ , the sample has entered into an insulating phase and no FQHE states are observed.

The most striking feature in this figure is the observation of a well-developed FQHE at  $\nu = 1/3$ . To our knowledge, this is the first time that the  $\nu = 1/3$  state has been observed in the Si/SiGe system. In  $\rho_{xx}$ , the minimum has reached a low value of  $\sim 50\Omega/\text{square}$ , and the temperature dependent measurements show that the  $\rho_{xx}$  is thermally activated. In  $\rho_{xy}$ , an apparent plateau

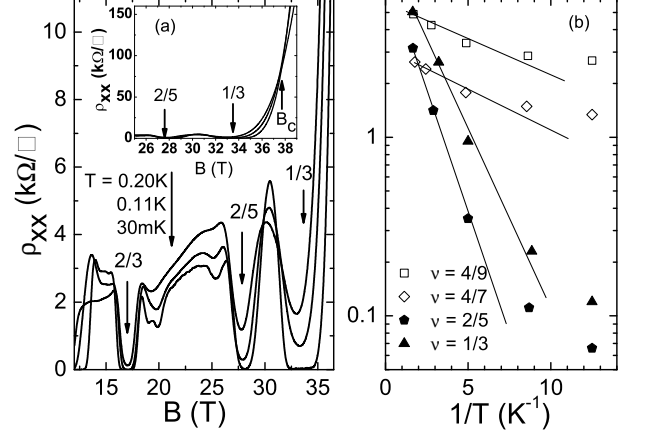


FIG. 2: (a)  $\rho_{xx}$  vs.  $B$  at selected temperatures. The inset shows the transition from the  $\nu = 1/3$  FQHE state to the high  $B$  insulating state. The critical  $B$  field is indicated by the arrow marked  $B_c$  and the critical resistivity is  $\rho_{xxc} \sim 80\text{k}\Omega/\text{square}$ . (b) Temperature dependence of  $\rho_{xx}$  minima of the FQHE states at  $\nu = 1/3$ ,  $2/5$ ,  $4/9$ , and  $4/7$ . Lines are linear fits to the data points and the energy gaps  $\Delta_{4/9} \sim \Delta_{4/7} \sim 0.2\text{K}$ ,  $\Delta_{1/3} \sim 0.8\text{K}$  and  $\Delta_{2/5} \sim 1.3\text{K}$ .

accompanies the  $\rho_{xx}$  minimum. We note that its quantization, however, is not exact. Since our sample is not patterned into a Hall bar, contact misalignment is likely to happen and the final value of  $\rho_{xy}$  may be contaminated with a component of  $\rho_{xx}$ . The usual method to show and eliminate this  $\rho_{xx}$  mixing effect is to reverse the  $B$  field direction, which, unfortunately, could not be done with the hybrid magnet in our experiment. The mixing from the strongly increasing  $\rho_{xx}$ , as the insulating phase is approached, gives rise to the continuous drop of  $\rho_{xy}$  when the  $B$  field is further increased beyond  $\nu = 1/3$ .

Fig. 2a shows the temperature dependence of  $\rho_{xx}$  for  $\nu < 1$ . In Fig. 2b the  $\rho_{xx}$  minima at  $\nu = 1/3$ ,  $2/5$ ,  $4/9$ , and  $4/7$  are plotted as a function of  $1/T$  on a semi-log scale. For all four states,  $\rho_{xx}$  shows the thermally activated behavior, as expected, and the energy gaps for the  $\nu = 1/3$  and  $2/5$  states, obtained by fitting the linear portion of the data to  $\rho_{xx} \propto \exp(-\Delta/2k_B T)$ , are  $\Delta_{1/3} \sim 0.8\text{K}$  and  $\Delta_{2/5} \sim 1.3\text{K}$ . (For the  $\nu = 4/9$  and  $\nu = 4/7$  states, the linear range of the data is small and the estimated gaps are  $\Delta_{4/9} \sim \Delta_{4/7} \sim 0.2\text{K}$ .) Unlike in GaAs, here,  $\Delta_{1/3}$  is smaller than  $\Delta_{2/5}$ . We believe that this difference is due to the close proximity of the  $1/3$  state here to the high  $B$  field insulating phase.

The two sequences of FQHE states evolving toward  $\nu = 1/2$  from  $\nu = 2/3$ ,  $3/5$ , and  $4/7$ , and from  $\nu = 1/3$ ,  $2/5$ , and  $4/9$  follow the two-flux composite fermion series of  $\nu = p/(2p \pm 1)$ . It shows that the CF model still applies in our multi-valley strained Si system. In Fig. 3, we compare the  $\rho_{xx}$  data around  $\nu = 1/2$  (or  $B_{eff} = 0$ ) and that around  $B = 0$ . It is clear that there exists a one-to-one correspondence between the IQHE states and

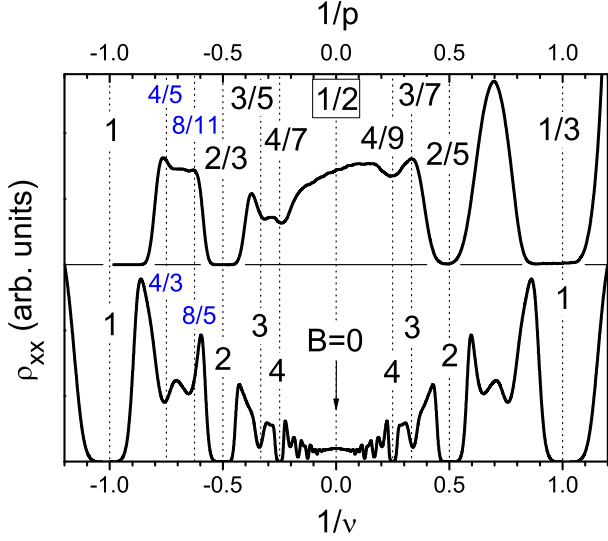


FIG. 3: Comparison of the two-flux CF series around  $\nu = 1/2$  and the IQHE states around  $B = 0$ . The IQHE trace was taken at an elevated temperature of  $T \sim 0.3\text{K}$ . The x-axis is  $1/\nu$  for electrons and  $1/p$  for CFs.

FQHE states — the positions of the  $\rho_{xx}$  minima and their relative strengths — for the same value of  $\nu$  and  $p$ . For example, the wide range of vanishing  $\rho_{xx}$  in the  $\nu = 1/3$  FQHE state corresponds to a similar range of vanishing  $\rho_{xx}$  in the  $\nu = 1$  IQHE state. A relatively weaker  $\nu = 2/5$  FQHE state corresponds to a less extended vanishing  $\rho_{xx}$  region of the  $\nu = 2$  IQHE state. More interestingly, the weak  $\nu = 3/5$  state (the missing  $\nu = 3/7$  state) when compared with the nearby  $\nu = 2/3$  and  $4/7$  states ( $\nu = 2/5$  and  $4/9$  states) resembles what is seen between  $\nu = 2$  and  $\nu = 4$  where the  $\nu = 3$  minimum is also the weakest. This similarity also appears in the temperature dependence (not shown). The fact that the  $\nu = 3/5$  FQHE state is more easily destroyed by raising the sample temperature than the  $\nu = 4/7$  state resembles again what has been observed in the IQHE regime, where the  $\nu = 3$  state also is more easily destroyed than the  $\nu = 4$  state. For the two weak minima at  $\nu = 4/5$  and  $8/11$ , they correspond to the FQHE states of electrons at  $\nu = 4/3$  and  $8/5$ . On the other hand, these two states can also be mapped to the IQHE states at  $p = 1$  and  $3$  of the CFs with four flux quanta forming at  $\nu = 3/4$ [16].

The similarity between the IQHE states and the FQHE states has long been seen in the GaAs/AlGaAs system and was, in fact, the primary motivation for the composite fermion model. It maps the FQHE of electrons onto the IQHE of CFs and thus naturally explains the one-to-one correspondence in the B field positions of  $\rho_{xx}$  minima. Moreover, the CF model is successful in explaining the relative strength of the FQHE states by relating their many-body energy gaps to the single-particle CF Landau level separations. Consequently, the larger  $p$  state, cor-

responding to a smaller CF Landau level separation, is generally weaker. However, it is not obvious whether this simple explanation still applies in the presence of other degree of freedom, for example, in our case the valley degeneracy. In the following, we show that, although a little bit more complicated, the relative strength of the FQHE in the strained Si can indeed be understood from the single-particle CF Landau level diagram.

First, we recall the physical origin of why the  $\nu = 3$  IQHE state is weaker than the nearby  $\nu = 2$  and  $4$  states. In strained (100) Si, where the two conduction valleys perpendicular to the surface are lower in energy, the strength of an IQHE state is determined by four energy scales — the Landau level separation ( $\hbar\omega_c$ ), its level broadening ( $\Gamma$ ), the Zeeman splitting ( $g\mu_B B$ ), and the valley splitting ( $\Delta_v$ ). The magnitude of  $\Delta_v$  is particularly important to the odd IQHE state. As shown schematically in the inset of Fig. 1, the energy gap of an odd IQHE state depends directly on  $\Delta_v$ . Since the valley splitting is generally smaller than the Landau level separation and Zeeman splitting, this explains why the  $\nu = 3$  state is weaker than the nearby  $\nu = 2$  and  $\nu = 4$  state. To estimate  $\Delta_v$ , we use the fact that the odd IQHE state appears when  $\Delta_v \geq \Gamma$ . For our specimen,  $\Gamma = \hbar/\tau = \hbar e/m\tau \sim 0.3\text{K}$ , where  $\tau$  is the transport lifetime,  $m = 0.2m_e$  is the effective mass of the electron, and  $\mu = 250,000\text{cm}^2/\text{Vs}$ . Based on our observation that the first resolved odd integer state is  $\nu = 11$ , we estimate  $\Delta_v \sim 0.3\text{K}$  at  $B = 1.0\text{T}$ .

In the FQHE regime, CFs form at  $\nu = 1/2[1, 2, 3, 4, 5, 6]$ . When  $B$  deviates from  $B_{1/2}$  (the  $B$  field at  $\nu = 1/2$ ), the CFs see a reduced effective  $B$  field,  $B_{\text{eff}} = B - B_{1/2}$ , and form Landau levels with a level separation of  $\hbar B_{\text{eff}}/m^*$  ( $m^*$  is the CF effective mass), giving rise to the IQHE of CFs. The IQHE state at Landau filling  $p$  of the CFs corresponds to the FQHE state of electrons at the filling  $\nu = p/(2p \pm 1)$ . To draw the CF Landau level diagram, again, we need to know the four energy scales — the CF Landau level separation ( $\hbar\omega_c^*$ ), its broadening ( $\Gamma^*$ ), the Zeeman splitting ( $E_z^*$ ), and the valley splitting ( $\Delta_v^*$ ). To estimate the Landau level separation, we use the effective mass,  $m^* \sim 1.4m_e$ , obtained from a scaling argument[16, 17, 18]. At  $p = 3$  (or  $\nu = 3/5$  and  $3/7$ ),  $\hbar\omega_c^* \sim 3\text{K}$ . The CF Landau level broadening  $\Gamma^* = \hbar e/m^*\mu^* \sim 1\text{K}$ , where  $\mu^*$  is the CF mobility. We calculate it from the resistivity at  $\nu = 1/2$ , using  $\mu^* = 1/ne\rho_{xx}(\nu = 1/2) \sim 7.5 \times 10^3\text{cm}^2/\text{Vs}$ . As to the CF Zeeman splitting, we recall that the effective  $g$ -factor of the CF is the same as that of the electron[19]. Consequently,  $E_z^* = g^*\mu_B B \sim 30\text{K}$ . Since  $E_z^* \gg \hbar\omega_c^*$ , the spin-degeneracy of the CF Landau level is completely lifted and the CFs can be viewed as spinless. Finally, from the similarity in  $\rho_{xx}$  between the CFs and the electrons, we conclude that at  $p = 3$  the two-fold valley degeneracy is also lifted for the CFs. Following the same criterion that  $\Delta_v^* \sim \Gamma^*$  for the first resolved odd IQHE state of the

CFs, we estimate a valley splitting  $\Delta_v^* \sim 1\text{K}$ .

Finally, a close examination of the temperature dependence of  $\rho_{xx}$  reveals a transition from the FQHE state at  $\nu = 1/3$  to an insulating state at higher  $B$  fields, as shown in the inset of Fig. 2a. The critical  $B$  field, at which the  $\rho_{xx}$  is temperature independent, is  $B_c \sim 37.6\text{T}$ , and the critical resistivity is  $\rho_{xxc} \sim 80\text{k}\Omega/\text{square}$ . This  $\rho_{xxc}$  is considerably larger than  $h/e^2 \sim 26\text{k}\Omega/\text{square}$ , observed in GaAs for the same transition[20].

To summarize, we have observed around  $\nu = 1/2$  the principal FQHE states, corresponding to the two-flux CF series  $p/(2p \pm 1)$ , at  $\nu = 2/3, 3/5, 4/7$ , and at  $\nu = 4/9, 2/5, 1/3$  in a high-mobility two-dimensional electron system in the strained Si layer of a (100)  $\text{Si}_{0.75}\text{Ge}_{0.25}/\text{Si}/\text{Si}_{0.75}\text{Ge}_{0.25}$  quantum well structure. The strengths of the two-flux CF series display a striking resemblance to those of the IQHE states of electrons, indicating that the two-fold degeneracy of the CF is lifted and an estimated valley splitting of  $\sim 1\text{K}$ . Our results show that the CF model still applies to the multi-valley Si/SiGe system.

This research was supported by the DOE and the NSF. The work at the NHMFL is supported by NSF Cooperative Agreement No. DMR-9527035 and by the State of Florida. Sandia is a multiprogram laboratory operated by Sandia Corporation, a Lockheed-Martin company, for the U.S. Department of Energy under Contract No. DE-AC04-94AL85000. We thank E. Palm, T. Murphy, S. Hannahs, B. Brandt, and the Hybrid Magnet operation team for their experimental assistances.

---

[1] J.K. Jain, Phys. Rev. Lett. **63**, 199 (1989).

[2] A. Lopez and E. Fradkin, Phys. Rev. B **44**, 5246 (1991).

[3] V. Kalmeyer and S.C. Zhang, Phys. Rev. B **46**, 9889 (1992).

[4] B.I. Halperin, P.A. Lee, and N. Read, Phys. Rev. B **47**, 7312 (1993).

[5] *Perspectives in Quantum Hall Effects*, edited by S. Das Sarma and A. Pinczuk (Wiley, New York, 1996).

[6] *Composite Fermions: A Unified View of the Quantum Hall Regime*, edited by O. Heinonen (World Scientific, Singapore, 1998).

[7] Y.H. Xie, E.A. Fitzgerald, D. Monroe, P.J. Silverman, and G.P. Waston, J. Appl. Phys. **73**, 8364 (1993).

[8] B.S. Meyerson, K.E. Ismail, D.L. Harame, F.K. LeGous, and J.M. Cstork, Semicond. Sci. Technol. **9**, 2005(1994).

[9] For a recent review of high mobility Si/SiGe structures, see, for example, F. Schaffler, Semicond. Sci. Technol. **12**, 1515 (1997).

[10] T. Okamoto, M. Ooya, K. Hosoya, and S. Kawaji, Phys. Rev. B **69**, 041202 (2004); A. Yutani and Y. Shiraki, Semicond. Sci. Technol. **11**, 1009 (1996).

[11] D. Monroe, Y.H. Xie, E.A. Fitzgerald, and P. J. Silverman, Phys. Rev. B **46**, 7935 (1992).

[12] S.F. Nelson, K. Ismail, J.J. Nocera, F.F. Fang, E.E. Mendez, J.O. Chu, and B.S. Meyerson, Appl. Phys. Lett. **61**, 64 (1992).

[13] R.B. Dunford, R. Newbury, F.F. Fang, R.G. Clark, R.P. Starrett, J.O. Chu, K.E. Ismail, and B.S. Meyerson, Solid State Commun. **96**, 57 (1995).

[14] K. Ismail, Physica B **227**, 310 (1996).

[15] P. Weitz, R.J. Haug, K. von. Klitzing, and F. Schaffler, Surf. Sci. **361**, 542 (1996).

[16] A.S. Yeh, H.L. Stormer, D.C. Tsui, L.N. Pfeiffer, K.W. Baldwin, and K.W. West, Phys. Rev. Lett. **82**, 592 (1999).

[17] Since the CF effective mass  $m^*$  is determined by electron-electron interaction, it scales as  $B_{1/2}$ . In the GaAs/AlGaAs system, it was found that  $m^*/m_e \sim 0.26 \times (B_{1/2})^{1/2} = 3.4 \times (B_{1/2})^{1/2}/\epsilon_{\text{GaAs}}$ [16, 18], where  $B_{1/2}$  is in units of Tesla and  $\epsilon_{\text{GaAs}}$  is the dielectric constant of GaAs. Replacing  $\epsilon_{\text{GaAs}}$  with  $\epsilon_{\text{Si}} = 11.7$  and  $B_{1/2} \sim 22.5\text{T}$ , we find  $m^* \sim 1.4m_e$ .

[18] R.R. Du, H.L. Stormer, D.C. Tsui, L.N. Pfeiffer, and K.W. West, Phys. Rev. Lett. **70**, 2944 (1993).

[19] R.R. Du, A.S. Yeh, H.L. Stormer, D.C. Tsui, L.N. Pfeiffer, and K.W. West, Phys. Rev. Lett. **75**, 3926 (1995).

[20] D. Shahar, D.C. Tsui, M. Shayegan, R.N. Bhatt, and J.E. Cunningham, Phys. Rev. Lett. **74**, 4511 (1995).